EPiC Series in Computing

Volume 80, 2021, Pages 161–175

8th International Workshop on Applied Verification of Continuous and Hybrid Systems (ARCH21)

Guaranteed State Estimation in CORA 2021

Matthias Althoff

Technical University of Munich,
Department of Informatics,
Munich, Germany
althoff@tum.de

Abstract

Tool presentation: Safety-critical systems often require guaranteed state estimation instead of estimating the most-likely state. While a lot of research on guaranteed state estimation has been conducted, there exists no tool for this purpose. Since guaranteed state estimation is in many cases a reachability problem or closely related to reachability analysis, this paper presents its implementation in the continuous reachability analyzer (CORA). We present how we integrated different types of observers, different set representations, and linear as well as nonlinear dynamics. The scalability and usefulness of the implemented observers is demonstrated for a scalable tank system.

1 Introduction

The knowledge of the state of a cyber-physical system is often indispensable for its control, prediction, and monitoring. Since typically not all states are measured—due to physical constraints or economic reasons—one often designs state observers to estimate the state of a system. Classical observer designs, such as Kalman filters, estimate the most likely state of a system. However, this is not sufficient for safety-critical systems for which one has to use guaranteed state estimation providing sets in which the state has to lie. These observers are also referred to as set-based observers. We will use the term *guaranteed state estimation* to emphasize that the true state can be enclosed and the term *set-based observers* to emphasize that this feature is realized by designing observers that compute with sets.

The knowledge of state bounds can be used for many applications. Robust control can use the set of possible states to ensure that the system will reach a goal region with certainty [17, 32, 38, 54, 66]. In fault tolerant control, the set of possible states can be used to reduce the false alarm rate in fault detection [13, 14, 21, 46, 47, 55–57, 60, 61]. Prediction algorithms are often used by autonomous systems to avoid conflicts with surrounding entities. To ensure safety, one has to start the prediction from the entire set of possible states [6, 44].

We survey the existing literature by categorizing set-based observers into three categories. The first category are strip-based observers, which propagate reachable sets and intersect them with strips of states possible from the current measurement. In essence, three operations are required: linear maps and Minkowski sum for the set propagation and intersection to correct

the sets based on measurements. This observer type has already been used in the 60s for linear time-invariant systems bounded by ellipsoids [53]. Since then, this approach has been improved by many researchers [11, 12, 18, 24, 29, 45]. The main disadvantage of using ellipsoids as a set representation is that they are not closed under Minkowski sum and intersection so that the obtained sets are often too over-approximative. Most recent strip-based observers use zonotopes since they are closed under linear maps and Minkowski sum; the computational complexity for linear maps is cubic and linear for Minkowski sums in the number of state variables [5, Tab. 1]. To the best knowledge of the author, the first paper proposing zonotopes for set-based observers is [20]. The subsequent approaches presented in the literature mostly differ in the way the intersection with strips is over-approximated [1, 34–37]. By extending zonotopes to constrained zonotopes, one not only inherits the computational complexity for linear maps, but also obtains exact intersections with strips [5, Tab. 1]. However, to obtain explicit bounds, one has to solve a linear program, so that this set representation is often not real-time capable when explicit bounds are required [55, eq. (25),(26)].

We refer to the second type of set-based observers as propagation-based observers. In essence, these observers evaluate Luenberger observers in a set-based fashion. Thus, these observers do not require intersections anymore and computing the set of possible states can be done by a reachability analysis of the Luenberger observer [22, 48]. The gain of the Luenberger observer can be computed online [22] of offline [64]. Most offline techniques ensure the stability by matrix inequalities so that this technique can typically only be applied to linear systems [57, 62, 64, 65].

The last category we review are interval observers. These observers compute the upper and lower bound for each state variable separately [25, 30, 43, 50, 67]. This can be done by, e.g., exploiting monotonicity of the system dynamics if possible [58, Sec. VI]. Since often the dynamics is not monotone, a new method is presented in [58, Alg. 1], which is proven to be at least as good as the classical interval observers exploiting monotonicity.

Although there exists a lot of research on set-based observers, there exists no tool for them—this is in contrast to reachability analysis, for which many tools have been implemented, see, e.g., [3, 9, 10, 15, 19, 26, 27, 49, 52]. By integrating set-based observers into CORA, we hope to make this fascinating method more accessible. Another contribution is to showcase the methodological overlap of reachability analysis and guaranteed state estimation, which should encourage more cross-fertilization of both disciplines. We have previously compared set-based observers of linear systems in [7]. In this work, we extend the comparison to nonlinear systems and focus more on the use of the tool rather than the underlying theory.

2 Types of Set-Based Observers

In principle, all observer types work for linear, nonlinear, and hybrid systems. However, to facilitate the introduction of different observer types, we limit ourselves in this section to linear discrete-time systems that are observable and time-invariant. Although this section is similar to [7, Sec. 2], we present the essence of each observer here as well for the convenience of the reader. Extensions to nonlinear systems are later discussed. We assume that the disturbance is bounded by the set $\mathcal{W}$ and the noise is bounded by the set $\mathcal{V}$. Using matrices A, B, and C of proper dimensions, the time step $k \in \mathbb{N}$, the state $x \in \mathbb{R}^n$, the measured output $y \in \mathbb{R}^m$, the disturbance vector $w \in \mathbb{R}^n$, and the sensor noise $v \in \mathbb{R}^m$, the system dynamics and measurement

function can be written as

$$\begin{aligned} x_{k+1} &= Ax_k + Bu_k + w_k, \\ y_k &= Cx_k + v_k. \end{aligned} \tag{1}$$

Please note that other works use $\tilde{E}\tilde{w}_k$ and $\tilde{F}\tilde{v}_k$ instead of w_k and v_k in (1). This, however, is covered by our form when simply choosing $\mathcal{W} = \tilde{E}\tilde{\mathcal{W}}$ and $\mathcal{V} = \tilde{F}\tilde{\mathcal{V}}$. One way to find appropriate sets $\mathcal{W}$ and $\mathcal{V}$ is to use conformance checking, see, e.g., [33, 39, 51]. To formalize the problem of set-based state estimation, we introduce the operator to receive the next state of (1) as $\chi(x_k, u_k, w_k)$. Our goal is to obtain the set of states $\mathcal{S}_k$ at time step k enclosing the true state from a set of initial states $\mathcal{S}_0 \subset \mathbb{R}^n$, which we define inductively:

$$\mathcal{S}_k = \left\{ x_k = \chi\Big(x_{k-1}, u_{k-1}, w_{k-1}\Big) \middle| x_{k-1} \in \mathcal{S}_{k-1}, w_{k-1} \in \mathcal{W}, v_k \in \mathcal{V}, y_k = Cx_k + v_k \right\}.$$

A reachability problem is a special case, which does not require to check the consistency with the measurement to obtain the reachable set as

$$\mathcal{R}_k = \left\{ x_k = \chi\Big(x_{k-1}, u_{k-1}, w_{k-1}\Big) \middle| x_{k-1} \in \mathcal{S}_{k-1}, w_{k-1} \in \mathcal{W} \right\}.$$

Please note that one often unifies u_k and w_k for reachability analysis by changing the system dynamics to $x_{k+1} = Ax_k + u_k$ and defining the set of possible inputs using the Minkowski sum[1] as $\mathcal{U}_k = Bu_k \oplus \mathcal{W}$. As we will see subsequently, set-propagation observers and interval observers reformulate the problem of guaranteed state estimation as a reachability problem, while strip-based observers combine reachability analysis with set intersection—similarly to guard intersections when computing reachable sets of hybrid systems [5].

2.1 Strip-Based Observers

Strip-based observers intersect the possible set of states according to the system dynamics with the set of states possible from the current measurement:

1. *Prediction*: We obtain the set of reachable states by evaluating (1) in a set-based fashion:

$$\mathcal{S}^p = A\mathcal{S}_{k-1} \oplus Bu_{k-1} \oplus \mathcal{W}.$$

2. *Measurement update*: The linear measurement function in (1) makes it possible to efficiently bound the state by measurements. To this end, let us introduce C_j as the j^{th} row of the measurement matrix C and the symmetric bound $[-\sigma, \sigma] = \text{BOX}(\mathcal{V})$ of the box enclosing the sensor noise. The possible states from the measurement of the j^{th} output signal $y_{k,j}$ at time step k are bounded by a strip of width σ_j [1, Property 2]:

$$\hat{\mathcal{S}}_j = \left\{ x \in \mathbb{R}^n \middle| |C_j x - y_{k,j}| \leq \sigma_j \right\}. \tag{2}$$

   The entire measurement set $\mathcal{S}_y$ is computed by over-approximatively intersecting all strips:

$$\hat{\mathcal{S}} \subseteq \hat{\mathcal{S}}_1 \cap \hat{\mathcal{S}}_2 \ldots \cap \hat{\mathcal{S}}_m. \tag{3}$$

[1] $\mathcal{A} \oplus \mathcal{B} = \{a + b | a \in \mathcal{A}, b \in \mathcal{B}\}$.

Algorithm 1 Interval observer from [58, Alg. 1].

Input: input sequence u_k, output sequence y_k
Output: sequence of state bounds $\underline{x}_k$, $\overline{x}_k$

1: $\hat{x}_0 \leftarrow \text{CENTER}(\mathcal{X}_0)$, $\quad \mathcal{D}_0 \leftarrow \mathcal{W} \oplus (-L)\mathcal{V}$
2: $\mathcal{S}_{x,0} \leftarrow \mathcal{X}_0$, $\quad \mathcal{S}_{wv,0} \leftarrow \mathbf{0}$
3: **for all** $k \geq 0$ **do**
4: $\quad [\underline{e}_k, \overline{e}_k] = \text{BOX}(\mathcal{S}_{x,k}) \oplus \mathcal{S}_{wv,k}$
5: $\quad [\underline{x}_k, \overline{x}_k] = \hat{x}_k + [\underline{e}_k, \overline{e}_k]$
6: $\quad \hat{x}_{k+1} = A\hat{x}_k + Bu_k + L(y_k - C\hat{x}_k)$
7: $\quad \mathcal{S}_{x,k+1} = (A - LC)\mathcal{S}_{x,k}$
8: $\quad \mathcal{S}_{wv,k+1} = \mathcal{S}_{wv,k} \oplus \text{BOX}(\mathcal{D}_k)$
9: $\quad \mathcal{D}_{k+1} = (A - LC)\mathcal{D}_k$
10: **end for**

3. *Correction*: The set consistent with the reachable set $\mathcal{S}^p$ and the measurement set $\hat{\mathcal{S}}$ is simply their intersection, which is often over-approximated for computational reasons [1, Sec.3]:

$$\mathcal{S}_k \supseteq \quad \mathcal{S}^p \cap \hat{\mathcal{S}}. \tag{4}$$

Next, we present set-propagation approaches, which do not require intersections.

2.2 Set-Propagation Observers

Because set-propagation approaches do not require intersections, one can more easily integrate set representations which are not closed under intersection, such as ellipsoids and zonotopes. These approaches are typically based on the update equation of a Luenberger observer:

$$\hat{x}_{k+1} = A\hat{x}_k + Bu_k + w_k + L(y_k - C\hat{x}_k - v_k), \tag{5}$$

where $\hat{x}$ is the estimated state and the observer gain L is designed such that the estimated state quickly converges to the true state. It is fairly easy to see that the set-based evaluation of (5) as

$$\mathcal{S}_{k+1} = (A - LC)\mathcal{S}_k \oplus Bu_k \oplus Ly_k \oplus (-L)\mathcal{V} \oplus \mathcal{W} \tag{6}$$

returns a guaranteed bound if $\hat{x}_0 \in \mathcal{S}_0$ and $\mathcal{V}$ as well as $\mathcal{W}$ contain the origin [22, Sec. 4.1]: The true solution is $x_{k+1} = Ax_k + Bu_k + w_k$ according to (5). Since $\mathcal{V}$ and $\mathcal{W}$ contain the origin, their set-based evaluation only inflates the true evolution of the state. Because this holds for any L, its values can be optimized for estimation accuracy—either offline (constant gain) or online (time-varying gain).

2.3 Interval Observers

As mentioned in the introduction, it has been shown in [58, Alg. 1] that there exists no interval observer with a better performance than the one presented in Alg. 1. This observer is based on (6) and avoids the wrapping effect by re-arranging the computation of (6) and using the box operator analogously to [28]. In essence, the estimated sets are represented by multi-dimensional intervals, which are split into their center $\hat{x}_k$ and the multi-dimensional error intervals $[\underline{e}_k, \overline{e}_k]$ (see line 5 of Alg. 1). The error intervals are composed of the boxed set $\text{BOX}(\mathcal{S}_{x,k})$ from the

homogeneous solution and the set $\mathcal{S}_{wv,k}$ bounding the input solution as shown in line 4 of Alg. 1. After replacing $\mathcal{S}_k$ in (6) with $\hat{x}_k \oplus \mathcal{S}_{x,k}$, we obtain the center in line 6 and the set of homogeneous solutions relative to $\hat{x}_{k+1}$ in line 7. The input solution is realized in line 8-9 using the same rearrangement presented in detail in [28].

2.4 Discussion

Because strip-based observers can only finish their computation of the estimated set $\mathcal{S}_k$ after the measurement y_k, their result is always delayed. When a set-propagation observer or interval observer is real-time capable, the set $\mathcal{S}_k$ is obtained ahead of time. This issue can be fixed for strip-based observers when additionally computing a one-step prediction and use this set as the initial set as shown in [54, Sec. III]. Since some practitioners may want to ignore the delayed computation (e.g. in fault-detection algorithms), we list the computation times in Sec. 4 without the additional prediction step, but list these algorithms as not ready for control. Interestingly, there exists a parameterization of both approaches such that exactly the same result is produced [62, Sec. 5] so that in this case, the propagation-based approach is clearly preferable.

3 Implemented Observers

The current list of observers implemented in CORA is presented in Tab. 1. The observers using zonotopes as a set representation are named by the cost function for bounding the states as tightly as possible. After defining a zonotope using the Minkowski sum and the r-dimensional unit box $\mathcal{B}^r = [-1, 1]^r$ as $\mathcal{Z} = c \oplus G\mathcal{B}^r$, we can define the used cost functions:

- **Volume:** The volume of a zonotope (see [1, Sec. 6.2]).
- **F_P-radius:** Given a symmetric weighting matrix $P \in \mathbb{R}^{n\times n}$, $P = P^T \succ 0$, the F_P-radius is the weighted Frobenius norm of G [22, Def. 2]:
$$F_P = \|G\|_{F,P} = \sqrt{\text{trace}(G^T P G)}.$$
Typically one chooses $P = I \in \mathbb{R}^{n\times n}$ and then just refers to this measure as the F-radius.
- **P-radius:** Given a positive definite matrix $P = P^T \succ 0$, the P-radius [37, Sec. 2] is
$$\Theta = \max_{z\in\mathcal{Z}}(\|z - c\|_P^2) = \max_{z\in\mathcal{Z}}\big((z - c)^T P(z - c)\big).$$

The observers implemented in CORA so far have been developed for linear systems. Approaches requiring an offline-computed observer gain cannot adapt to an over-approximative on-the-fly linearization of a nonlinear system. However, all other approaches have been extended to nonlinear systems by using an over-approximated on-the-fly linearization of the nonlinear dynamics at every time step k. This works well in practice, as shown in the numerical experiments in Sec. 4, however, one can no longer guarantee that the set of estimated states converges. By adding a fail-safe layer as, e.g., proposed in our previous works [4, 54], one can ensure a safe operation even in the event that the set of estimated states grows unacceptably large.

To demonstrate how easy it is to obtain estimated states with guaranteed bounds, we provide an example that implements the observer in [1, Sec. 7.1]. The subsequent code produces the plots of the state bounds over time shown in Fig. 1. A more in-depth analysis of the implemented observers is presented in the subsequent section for a scalable water tank system.

Table 1: Set-based observers currently implemented in CORA.

Technique	Set representation	Ready for control	Supported dynamics	Reference
strip-based observers				
VolMin-A	zonotope	✗	linear/nonlinear	[1]
VolMin-B	zonotope	✗	linear/nonlinear	[16]
FRad-A	zonotope	✗	linear/nonlinear	[1]
FRad-B	zonotope	✗	linear/nonlinear	[62]
PRad-A	zonotope	✗	linear	[37]
PRad-B	zonotope	✗	linear	[36]
PRad-C	zonotope	✗	linear	[59]
PRad-D	zonotope	✗	linear	[63]
CZN-A	constr. zono.	✗	linear/nonlinear	[55]
CZN-B	constr. zono.	✗	linear/nonlinear	[2]
ESO-A	ellipsoid	✗	linear	[29, 40]
ESO-B	ellipsoid	✗	linear	[40]
set-propagation observers				
FRad-C	zonotope	✓	linear/nonlinear	[22]
PRad-E	zonotope	✓	linear	[64]
Nom-G	zonotope	✓	linear	[62]
ESO-C	ellipsoid	✓	linear	[41]
ESO-D	ellipsoid	✓	linear	[42]
interval observer				
Hinf-G	zonotope	✓	linear	[58]

```
%% Parameters
params.tFinal = 20; % final time
params.R0 = zonotope(zeros(2,1),3*eye(2)); % initial set
params.V = 0.2*zonotope([0,1]); % sensor noise set
params.W = 0.02*[-6; 1]*zonotope([0,1]); % disturbance set
params.uTransVec = zeros(2,1e3); % input vector
params.yVec = [0.79, 5.00, 4.35, 1.86, -0.11, -1.13, -1.17, -0.76, ...
    -0.12, 0.72, 0.29, 0.19, 0.09, -0.21, 0.05, -0.00, -0.16, 0.01, ...
    -0.08, 0.13]; % measurement vector


%% Algorithmic Settings
options.zonotopeOrder = 20; % zonotope order
options.timeStep = 1; % step size
options.alg = 'FRad-C'; % observer approach

%% System Dynamics
A = [0 -0.5; 1 1];
B = 1;
c = zeros(2,1);
C = [-2 1];
sys = linearSysDT('sys',A, B, c, C, options.timeStep);

%% Observe
EstSet = observe(sys,params,options);

%% Plot Results
for iDim = 1:2
    figure; hold on;
```

```
    % plot time elapse
    plotOverTime(EstSet,iDim,'FaceColor',[.6 .6 .6],'EdgeColor','none');

    % label plot
    xlabel('t');
    ylabel(['x_{',num2str(iDim),'}']);
end
```

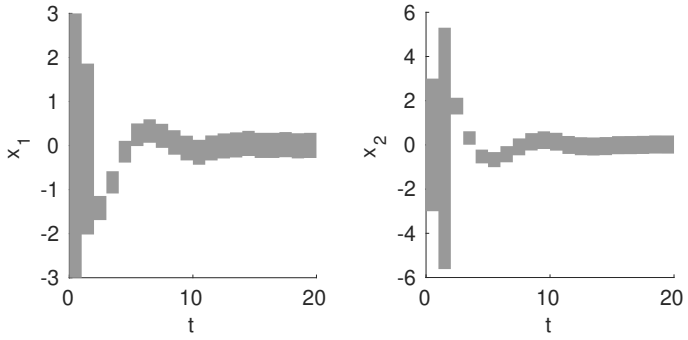

Figure 1: State bounds for the example in [1, Sec. 7.1].

4 Numerical Experiments

To investigate the scalability of the implemented methods, we are testing them on a water tank system shown in Fig. 2 to which one can add arbitrarily many tanks. This example is inspired by [8] and could, e.g., model the water levels in between hydroelectric power stations. The state vector x consists of the water levels of each tank, u is the water inflow vector, and w is the disturbance vector. To obtain the i^{th} element of an expression in parentheses, we use the notation $(\cdot)_i$. After introducing the cross-sectional area A_i of the i^{th} tank and the corresponding cross-sectional area of the outflow κ_i, the differential equation for the water level of the first tank is given by Toricelli's law [23]:

$$\dot{x}_1 = \frac{1}{A_1}\big(-\kappa_1\sqrt{2gx_1} + (Bu+w)_1\big).$$

The differential equation for the ith tank is

$$\dot{x}_i = \frac{1}{A_i}\big(\kappa_{i-1}\sqrt{2gx_{i-1}} - \kappa_i\sqrt{2gx_i} + (Bu+w)_i\big).$$

To obtain a discrete-time model, we simply assume that the flow is constant for one time step of duration $h = t_{k+1} - t_k$ so that we obtain

$$x_{k+1,1} = x_{k,1} + \frac{h}{A_1}\big(-\kappa_1\sqrt{2gx_{k,1}} + (Bu_k + w_k)_1\big)$$

for the first tank and

$$x_{k+1,i} = x_{k+1,i} + \frac{h}{A_i}\big(\kappa_{i-1}\sqrt{2gx_{k,i-1}} - \kappa_i\sqrt{2gx_{k,i}} + (Bu_k + w_k)_i\big)$$

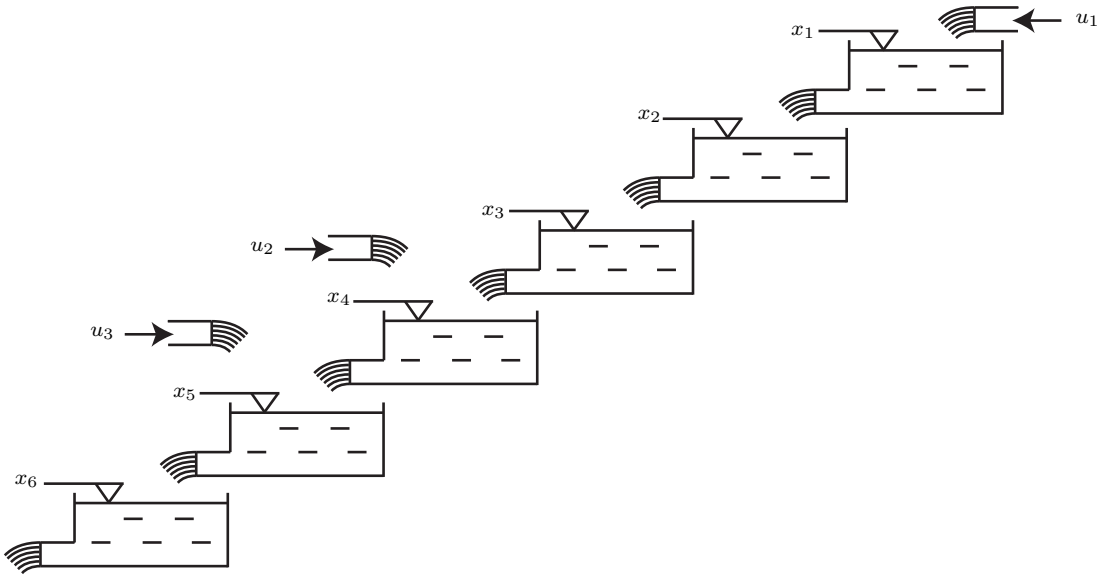

Figure 2: Tank system.

Table 2: Indices of tanks with water inflow and water level measurement.

	tank indices
water inflow	1, 4, 5, 7, 9, 10, 13, 15, 16, 19, 21, 22, 25, 27, 28
water level measurement	2, 4, 5, 7, 8, 10, 11, 13, 14, 16, 17, 19, 20, 21, 22, 23, 25, 26, 27, 28, 29

for all other tanks. For simplicity, all parameters are chosen to be identical for all tanks. The cross section of the tanks is $A_i = 1$ [m^2], the cross section of the outflow is $\kappa_i = 0.015$ [m^2], the time step is $h = 0.5$ [s], the initial set is bounded by $x_i(0) \in [16, 24]$ [m], the disturbance is bounded by $w_i \in [-1, 1] \cdot 10^{-3}$ [m^3/s], and the measurement noise is bounded by $v_i \in [-0.2, 0.2]$ [m]. The list of tanks that are measured and have water inflow for the 30-tank system is presented in Tab. 2. Smaller tank systems have the same configuration, with the trivial difference that tank indices beyond the number of tanks are ignored. The water inflow trajectory $u(.)$ is not presented since it only has a minor effect on the performance of the set-based observers; besides, its presentation would be space-consuming and thus is only provided in CORA 2021.

We evaluate all observers with respect to tightness of the estimated sets and computation time. Since computing the volume is infeasible for many dimensions [31], the relative root-mean-square (rms) values of the interval radius $r_{i,k,l}$ of the i^{th} state variable at step k out of N time steps of observer l are computed as:

$$v_{i,l} = \frac{\tilde{r}_{i,l}}{\min(\tilde{r}_{i,1}, \ldots, \tilde{r}_{i,n_l})}, \; \tilde{r}_{i,l} = \sqrt{\left(\frac{1}{N}\sum_{k=0}^{N-1} r_{i,k,l}^2\right)}. \tag{7}$$

All computations were performed on an Intel(R) Core(TM) i7-8565U CPU @ 1.80GHz with MATLAB 2020b with single thread executions. The code for the comparison is available in CORA (cora.in.tum.de). Some results for the 30-tank system when using the FRad-C technique are shown in Fig. 3 together with the true state.

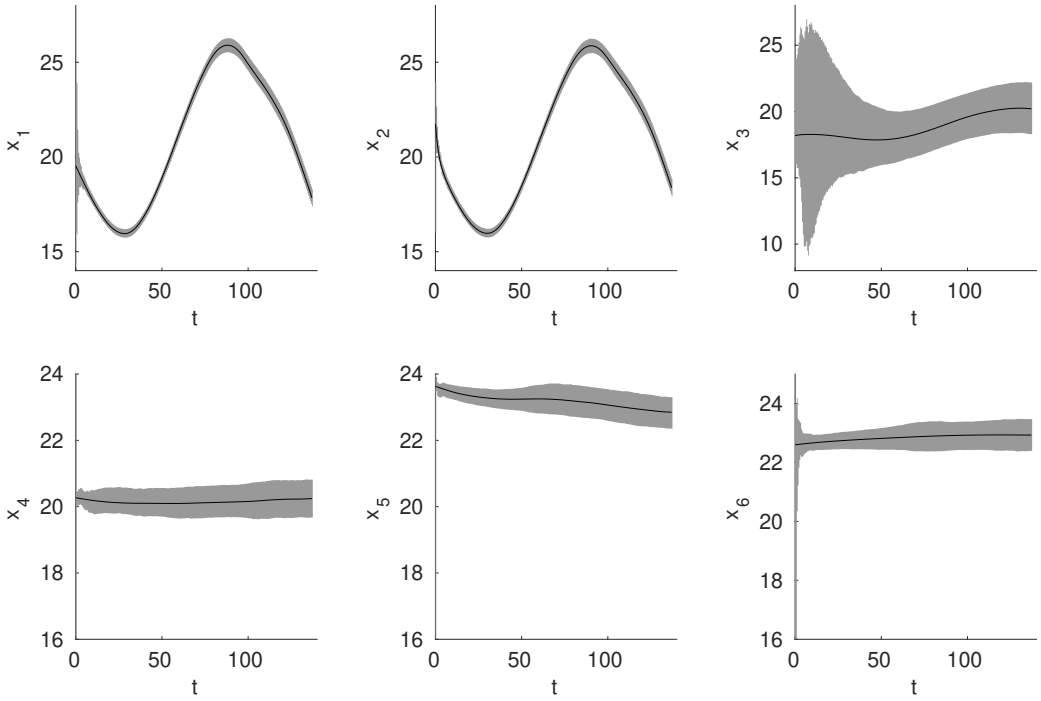

Figure 3: State bounds for the first six tanks of the 30-tank example when using the FRad-C approach.

The results for the linearized six-tank system and the original dynamics are shown in Tab. 3 and 4, respectively. For the higher-dimensional problems, we cannot present the rms values of the interval radii of all dimensions due to space limitations. Instead, we only present the average result across all dimensions and the computation times for the linearized and the original dynamics in Tab. 3 and 4, respectively.

It can be seen that all observers are real-time capable since new measurements are collected every 500 [ms]. Another obvious observation is that approaches using zonotopes obtain tighter results compared to approaches using ellipsoids. For strip-based observers, most approaches using zonotopes were not only more precise, but also faster than the approaches using ellipsoids. In contrast, the investigated ellipsoidal techniques for set-propagation observers (ESO-C and ESO-D) were significantly faster. The considered interval observer (Hinf-G) is filling the gap between high accuracy and low computational costs: In terms of accuracy and computation time it is between the group ESO-C and ESO-D and the remaining observers—only PRad-A had a worse accuracy.

Table 3: Linearized 6-tank system: Relative rms values v_i according to (7) and their average (avg). Indices of unmeasured states: $1, 3, 6$. Indices of measured states: $2, 4, 5$.

technique	set representation	in time	v_1	v_2	v_3	v_4	v_5	v_6	avg	t_c [ms]
strip-based observers										
VolMin-B	zonotope	✗	1.000	1.182	1.000	1.029	1.692	1.011	1.152	298.7
FRad-A	zonotope	✗	1.060	1.293	1.428	1.862	1.344	1.002	1.332	0.885
FRad-B	zonotope	✗	1.396	1.277	1.457	1.823	1.307	1.006	1.378	0.748
PRad-A	zonotope	✗	6.314	9.302	6.882	6.258	1.157	1.415	5.221	0.995
PRad-B	zonotope	✗	2.230	1.171	2.351	1.171	1.114	1.005	1.507	0.536
PRad-C	zonotope	✗	2.220	1.000	1.728	1.007	1.000	1.004	1.326	0.422
PRad-D	zonotope	✗	2.335	1.016	1.430	1.000	1.004	1.004	1.298	0.447
ESO-A	ellipsoid	✗	15.42	27.09	3.576	29.54	28.84	2.584	17.84	1.014
ESO-B	ellipsoid	✗	12.39	21.34	3.482	19.55	16.50	2.516	12.63	0.864
set-propagation observers										
FRad-C	zonotope	✓	1.272	1.843	1.430	2.264	1.822	1.002	1.605	0.594
PRad-E	zonotope	✓	2.321	2.016	2.165	1.747	1.691	1.000	1.823	0.411
Nom-G	zonotope	✓	2.414	1.955	1.545	1.613	1.590	1.000	1.686	0.366
ESO-C	ellipsoid	✓	37.11	61.53	4.287	57.65	59.49	2.549	37.10	0.046
ESO-D	ellipsoid	✓	39.81	66.01	4.598	61.85	63.81	2.734	39.80	0.039
interval observer										
Hinf-G	zonotope	✓	2.631	2.581	1.711	2.210	2.166	1.027	2.055	0.227
smallest absolute radii										
			0.3596	0.2036	1.940	0.2019	0.2004	2.737		

Table 4: Nonlinear 6-tank system: Relative rms values v_i according to (7) and their average (avg). Indices of unmeasured states: $1, 3, 6$. Indices of measured states: $2, 4, 5$.

technique	set representation	in time	v_1	v_2	v_3	v_4	v_5	v_6	avg	t_c [ms]
strip-based observers										
VolMin-B	zonotope	✗	1.000	1.000	1.000	1.000	1.316	1.010	1.054	385.2
FRad-A	zonotope	✗	1.027	1.019	1.527	1.869	1.000	1.000	1.240	3.938
FRad-B	zonotope	✗	1.358	1.004	1.576	1.867	1.013	1.004	1.304	5.202
set-propagation observers										
FRad-C	zonotope	✓	1.228	1.427	1.523	2.237	1.358	1.000	1.462	3.848
smallest absolute radii										
			0.3795	0.2647	2.117	0.2082	0.2661	2.837		

The above-mentioned observations are amplified for larger systems. The ellipsoidal techniques become increasingly inaccurate and the average of rms errors over all states is in some cases more than 50 times higher. It should also be noted that we could only find gains for the PRad-A technique when the system had 12 or less tanks and the solution for the 12-tank system was already instable. Due to numerical issues, we also could not compute the solution of the ESO-B approach for the 18-tank system. A particular good ratio of accuracy and efficiency for the linear use case was achieved by PRad-B, PRad-C, and PRad D.

Table 5: Scalability of the implemented techniques for linear systems. The average (avg) of the rms values υ_i according to (7) and the computation times t_c in [ms] are shown.

technique	set representation	in time	12 tanks		18 tanks		24 tanks		30 tanks	
			avg	t_c	avg	t_c	avg	t_c	avg	t_c
strip-based observers										
VolMin-B	zonotope	✗	1.413	1409	-	-	-	-	-	-
FRad-A	zonotope	✗	1.799	1.997	1.611	3.708	1.550	6.586	1.559	14.94
FRad-B	zonotope	✗	1.835	0.994	1.655	1.253	1.609	1.833	1.594	2.675
PRad-A	zonotope	✗	Inf	-	noGain	-	noGain	-	noGain	-
PRad-B	zonotope	✗	2.035	0.859	1.501	1.136	1.280	1.444	1.262	2.108
PRad-C	zonotope	✗	1.662	0.771	1.294	1.040	1.153	1.454	1.130	2.427
PRad-D	zonotope	✗	1.515	1.085	1.258	1.119	1.144	1.522	1.399	1.989
ESO-A	ellipsoid	✗	22.78	2.822	29.49	2.299	32.33	8.543	35.09	9.004
ESO-B	ellipsoid	✗	14.16	1.176	NaN	-	17.70	5.424	22.02	7.517
set-propagation observers										
FRad-C	zonotope	✓	2.039	0.977	1.888	1.049	1.878	1.765	1.879	2.654
PRad-E	zonotope	✓	2.242	0.687	1.859	0.878	1.716	1.309	1.703	1.748
Nom-G	zonotope	✓	1.911	0.614	1.711	1.076	1.615	1.309	1.610	1.936
ESO-C	ellipsoid	✓	5.268	0.036	10.84	0.047	20.09	0.026	29.40	0.034
ESO-D	ellipsoid	✓	35.07	0.033	42.92	0.039	60.42	0.035	73.41	0.035
interval observer										
Hinf-G	zonotope	✓	2.337	0.330	2.081	0.465	1.971	0.708	1.952	1.304

Table 6: Scalability of the implemented techniques for nonlinear systems. The average (avg) of the rms values υ_i according to (7) and the computation times t_c in [ms] are shown.

technique	set representation	in time	12 tanks		18 tanks		24 tanks		30 tanks	
			avg	t_c	avg	t_c	avg	t_c	avg	t_c
strip-based observers										
VolMin-B	zonotope	✗	1.184	3451	-	-	-	-	-	-
FRad-A	zonotope	✗	1.259	10.60	1.002	19.51	1.005	23.22	1.002	36.43
FRad-B	zonotope	✗	1.314	8.273	1.071	13.21	1.062	20.05	1.072	22.65
set-propagation observers										
FRad-C	zonotope	✓	1.482	9.043	1.196	12.45	1.207	20.29	1.223	21.46

For the nonlinear use case, we could only directly apply the approaches minimizing the F-radius and the volume minimization. As mentioned before, volume computation and volume approximation are computationally expensive so that only the F-radius techniques can be used for higher-dimensional problems. Since all F-radius techniques compute with zonotopes, the results are very similar for all F-radius approaches (FRad-A, FRad-B, FRad-C). Interestingly, although FRad-C is a set propagation technique, the performance is similar to the techniques using strip intersections. The FRad-C technique additionally has the advantage that the results are obtained in time and are not delayed as for strip-based observers.

5 Conclusions

This paper presents the first tool for set-based observers for linear and nonlinear systems using various set representations. Obviously, constrained zonotopes ensure the most accurate results since they are closed under all required operations, but they are often not real-time capable when one requires explicit bounds. In contrast, zonotopes are often real-time capable and typically more accurate than ellipsoids. If only a very basic microcontroller can be used, ellipsoidal observers might be the best choice due to the smallest possible computation times. By sharing as much code as possible for different observer types, the implementation is easy to maintain. We also added several unit tests and all required set operations are already implemented in CORA since many years, helping to ensure a good code quality. Due to the similarities between reachability analysis and set-based observers, one can be hopeful that both research communities have a more intensive exchange in the future.

Acknowledgment

The author gratefully acknowledges financial support by the European Commission project justITSELF under grant number 817629.

References

[1] T. Alamo, J. M. Bravo, and E. F. Camacho. Guaranteed state estimation by zonotopes. *Automatica*, 41(6):1035–1043, 2005.

[2] A. Alanwar, V. Gassmann, X. He, H. Said, H. Sandberg, K. H. Johansson, and M. Althoff. Privacy preserving set-based estimation using partially homomorphic encryption, 2020. arXiv:2010.11097.

[3] M. Althoff. An introduction to CORA 2015. In *Proc. of the Workshop on Applied Verification for Continuous and Hybrid Systems*, page 120–151, 2015.

[4] M. Althoff and J. M. Dolan. Online verification of automated road vehicles using reachability analysis. *IEEE Transactions on Robotics*, 30(4):903–918, 2014.

[5] M. Althoff, G. Frehse, and A. Girard. Set propagation techniques for reachability analysis. *Annual Review of Control, Robotics, and Autonomous Systems*, 4(1):369–395, 2021.

[6] M. Althoff and S. Magdici. Set-based prediction of traffic participants on arbitrary road networks. *IEEE Transactions on Intelligent Vehicles*, 1(2):187–202, 2016.

[7] M. Althoff and J. J. Rath. Comparison of guaranteed state estimators for linear time-invariant systems. *Automatica*, 130, 2021. article no. 109662.

[8] M. Althoff, O. Stursberg, and M. Buss. Reachability analysis of nonlinear systems with uncertain parameters using conservative linearization. In *Proc. of the 47th IEEE Conference on Decision and Control*, page 4042–4048, 2008.

[9] S. Bak and P. S. Duggirala. HyLAA: A tool for computing simulation-equivalent reachability for linear systems. In *Proc. of the 20th International Conference on Hybrid Systems: Computation and Control*, page 173–178, 2017.

[10] L. Benvenuti, D. Bresolin, P. Collins, A. Ferrari, L. Geretti, and T. Villa. Assume-guarantee verification of nonlinear hybrid systems with ARIADNE. *International Journal of Robust and Nonlinear Control*, 24:699–724, 2014.

[11] D. P. Bertsekas and I. B. Rhodes. Recursive state estimation for a set-membership description of uncertainty. *IEEE Transactions on Automatic Control*, 16:117–128, 1971.

[12] F. Blanchini and S. Miani. *Set-theoretic estimation*, page 527–551. Springer, 2015.

[13] J. Blesa, V. Puig, J. Romera, and J. Saludes. Fault diagnosis of wind turbines using a set-membership approach. *IFAC Proceedings Volumes*, 44(1):8316–8321, 2011.

[14] J. Blesa, D. Rotondo, V. Puig, and F. Nejjari. FDI and FTC of wind turbines using the interval observer approach and virtual actuators/sensors. *Control Engineering Practice*, 24:138–155, 2014.

[15] S. Bogomolov, M. Forets, G. Frehse, K. Potomkin, and C. Schilling. JuliaReach: A toolbox for set-based reachability. page 39–44, 2019.

[16] J. M. Bravo, T. Alamo, and E. F. Camacho. Bounded error identification of systems with time-varying parameters. *IEEE Transactions on Automatic Control*, 51(7):1144–1150, 2006.

[17] J. M. Bravo, T. Alamo, and E. F. Camacho. Robust MPC of constrained discrete-time nonlinear systems based on approximated reachable sets. *Automatica*, 42:1745–1751, 2006.

[18] S. B. Chabane. *Fault detection techniques based on set-membership state estimation for uncertain systems*. Dissertation, Université Paris-Saclay, 2015.

[19] X. Chen, E. Ábrahám, and S. Sankaranarayanan. Flow*: An analyzer for non-linear hybrid systems. In *Proc. of Computer-Aided Verification*, LNCS 8044, page 258–263. Springer, 2013.

[20] C. Combastel. A state bounding observer based on zonotopes. In *Proc. of the European Control Conference*, page 2589–2594, 2003.

[21] C. Combastel. Merging Kalman filtering and zonotopic state bounding for robust fault detection under noisy environment. *IFAC-PapersOnLine*, 48(21):289–295, 2015.

[22] C. Combastel. Zonotopes and Kalman observers: Gain optimality under distinct uncertainty paradigms and robust convergence. *Automatica*, 55:265–273, 2015.

[23] R. D. Driver. Torricelli's law–an ideal example of an elementary ODE. *The American Mathematical Monthly*, 105(5):453–455, 1998.

[24] C. Durieu, É. Walter, and B. Polyak. Multi-input multi-output ellipsoidal state bounding. *Journal of Optimization Theory and Applications*, 111(2):273–303, 2001.

[25] D. Efimov, T. Raïssi, S. Chebotarev, and A. Zolghadri. Interval state observer for nonlinear time varying systems. *Automatica*, 49(1):200–205, 2013.

[26] C. Fan, B. Qi, S. Mitra, M. Viswanathan, and P. S. Duggirala. Automatic reachability analysis for nonlinear hybrid models with C2E2. In *Computer Aided Verification*, page 531–538, 2016.

[27] G. Frehse, C. Le Guernic, A. Donzé, S. Cotton, R. Ray, O. Lebeltel, R. Ripado, A. Girard, T. Dang, and O. Maler. SpaceEx: Scalable verification of hybrid systems. In *Proc. of the 23rd International Conference on Computer Aided Verification*, LNCS 6806, page 379–395. Springer, 2011.

[28] A. Girard, C. Le Guernic, and O. Maler. Efficient computation of reachable sets of linear time-invariant systems with inputs. In *Hybrid Systems: Computation and Control*, LNCS 3927, page 257–271. Springer, 2006.

[29] S. Gollamudi, S. Nagaraj, S. Kapoor, and Y. F. Huang. Set-membership state estimation with optimal bounding ellipsoids. In *Proc. of the International Symposium on Information Theory and its Applications*, page 262–265, 1996.

[30] J. L. Gouzé, A. Rapaport, and M. Z. Hadj-Sadok. Interval observers for uncertain biological systems. *Ecological Modelling*, 133(1):45–56, 2000.

[31] E. Gover and N. Krikorian. Determinants and the volumes of parallelotopes and zonotopes. *Linear Algebra and its Applications*, 433(1):28–40, 2010.

[32] F. Gruber and M. Althoff. Scalable robust model predictive control for linear sampled-data systems. In *Proc. of the 58th IEEE Conference on Decision and Control*, page 438–444, 2019.

[33] N. Kochdumper, A. Tarraf, M. Rechmal, M. Olbrich, L. Hedrich, and M. Althoff. Establishing reachset conformance for the formal analysis of analog circuits. In *Proc. of the 25th Asia and South Pacific Design Automation Conference*, page 199–204, 2020.

[34] V. T. H. Le, T. Alamo, E. F. Camacho, C. Stoica, and D. Dumur. A new approach for guaranteed state estimation by zonotopes. page 9242–9247, 2011.

[35] V. T. H. Le, T. Alamo, E. F. Camacho, C. Stoica, and D. Dumur. Zonotopic set-membership estimation for interval dynamic systems. In *Proc. of the IEEE American Control Conference*, page 6787–6792, 2012.

[36] V. T. H. Le, C. Stoica, T. Alamo, E. F. Camacho, and D. Dumur. Zonotope-based set-membership estimation for multi-output uncertain systems. In *Proc. of the IEEE International Symposium on Intelligent Control*, page 212–217, 2013.

[37] V. T. H. Le, C. Stoica, T. Alamo, E. F. Camacho, and D. Dumur. Zonotopic guaranteed state estimation for uncertain systems. *Automatica*, 49(11):3418–3424, 2013.

[38] V. T. H. Le, C. Stoica, D. Dumur, T. Alamo, and E. F. Camacho. Robust tube-based constrained predictive control via zonotopic set-membership estimation. In *Proc. of the IEEE Conference on Decision and Control and European Control Conference*, page 4580–4585, 2011.

[39] S. B. Liu and M. Althoff. Reachset conformance of forward dynamic models for the formal analysis of robots. In *Proc. of the IEEE/RSJ International Conference on Intelligent Robots and Systems*, page 370–376, 2018.

[40] Y. Liu, Y. Zhao, and F. Wu. Ellipsoidal state-bounding-based set-membership estimation for linear system with unknown-but-bounded disturbances. *IET Control Theory & Applications*, 10(4):431–442, 2016.

[41] N. Loukkas, J. J. Martinez, and N. Meslem. Set-membership observer design based on ellipsoidal invariant sets. *IFAC-PapersOnLine*, 50(1):6471–6476, 2017.

[42] J. J. Martinez, N. Loukkas, and N. Meslem. H-infinity set-membership observer design for discrete-time LPV systems. *International Journal of Control*, 93(10):2314–2325, 2020.

[43] F. Mazenc and O. Bernard. Interval observers for linear time-invariant systems with disturbances. *Automatica*, 47(1):140–147, 2011.

[44] A. Pereira and M. Althoff. Overapproximative human arm occupancy prediction for collision avoidance. *IEEE Transactions on Automation Science and Engineering*, 15(2):818–831, 2018.

[45] B. T. Polyak, S. A. Nazin, C. Durieu, and E. Walter. Ellipsoidal parameter or state estimation under model uncertainty. *Automatica*, 40(7):1171–1179, 2004.

[46] M. Pourasghar, V. Puig, and C. Ocampo-Martinez. Interval observer versus set-membership approaches for fault detection in uncertain systems using zonotopes. *International Journal of Robust and Nonlinear Control*, 29(10):2819–2843, 2019.

[47] V. Puig. Fault diagnosis and fault tolerant control using set-membership approaches: Application to real case studies. *International Journal of Applied Mathematics and Computer Science*, 20:619–635, 2010.

[48] V. Puig, P. Cuguero, and J. Quevedo. Worst-case state estimation and simulation of uncertain discrete-time systems using zonotopes. In *Proc. of the IEEE European Control Conference*, page 1691–1697, 2001.

[49] R. Ray, A. Gurung, B. Das, E. Bartocci, S. Bogomolov, and R. Grosu. XSpeed: Accelerating reachability analysis on multi-core processors. In *Hardware and Software: Verification and Testing*, page 3–18. Springer International Publishing, 2015.

[50] T. Raïssi and D. Efimov. Some recent results on the design and implementation of interval observers for uncertain systems. *Automatisierungstechnik*, 66(3):213–224, 2018.

[51] H. Roehm, J. Oehlerking, M. Woehrle, and M. Althoff. Model conformance for cyber-physical systems: A survey. *ACM Transactions on Cyber-Physical Systems*, 3(3):Article 30, 2019.

[52] S. Schupp, E. Abraham, I. Ben Makhlouf, and S. Kowalewski. HyPro: A C++ library for state set representations for hybrid systems reachability analysis. In *Proc. of the NASA Formal Methods Symposium*, page 288–294, 2017.

[53] F. Schweppe. Recursive state estimation: Unknown but bounded errors and system inputs. *IEEE Transactions on Automatic Control*, 13(1):22–28, 1968.

[54] B. Schürmann, N. Kochdumper, and M. Althoff. Reachset model predictive control for disturbed nonlinear systems. In *Proc. of the 57th IEEE Conference on Decision and Control*, page 3463–3470, 2018.

[55] J. K. Scott, D. M. Raimondo, G. R. Marseglia, and R. D. Braatz. Constrained zonotopes: A new tool for set-based estimation and fault detection. *Automatica*, 69:126–136, 2016.

[56] J. Su and W. Chen. Model-based fault diagnosis system verification using reachability analysis. *IEEE Transactions on Systems, Man, and Cybernetics: Systems*, 49(4):742–751, 2019.

[57] W. Tang, Z. Wang, Y. Shen, M. Rodrigues, and D. Theilliol. Fault detection based on multi-objective observer and interval hull computation. *IFAC-PapersOnLine*, 51(24):332–337, 2018.

[58] W. Tang, Z. Wang, Y. Wang, T. Raïssi, and Y. Shen. Interval estimation methods for discrete-time linear time-invariant systems. *IEEE Transactions on Automatic Control*, 64(11):4717–4724, 2019.

[59] Y. Wang, T. Alamo, V. Puig, and G. Cembrano. A distributed set-membership approach based on zonotopes for interconnected systems. In *Proc. of the IEEE Conference on Decision and Control*, page 668–673, 2018.

[60] Y. Wang and V. Puig. Zonotopic extended Kalman filter and fault detection of discrete-time nonlinear systems applied to a quadrotor helicopter. In *Proc. of the 3rd IEEE Conference on Control and Fault-Tolerant Systems*, page 367–372, 2016.

[61] Y. Wang, V. Puig, and G. Cembrano. Robust fault estimation based on zonotopic Kalman filter for discrete-time descriptor systems. *International Journal of Robust and Nonlinear Control*, 28(16):5071–5086, 2018.

[62] Y. Wang, V. Puig, and G. Cembrano. Set-membership approach and Kalman observer based on zonotopes for discrete-time descriptor systems. *Automatica*, 93:435–443, 2018.

[63] Y. Wang, Z. Wang, V. Puig, and G. Cembrano. Zonotopic set-membership state estimation for discrete-time descriptor LPV systems. *IEEE Transactions on Automatic Control*, 64(5):2092–2099, 2019.

[64] Y. Wang, M. Zhou, V. Puig, G. Cembrano, and Z. Wang. Zonotopic fault detection observer with $\mathcal{H}_-$ performance. In *Proc. of the 36th IEEE Chinese Control Conference*, page 7230–7235, 2017.

[65] Z. Wang, W. Tang, Q. Zhang, V. Puig, and Y. Shen. Zonotopic state estimation and fault detection for systems with time-invariant uncertainties. *IFAC-PapersOnLine*, 51(24):494–499, 2018.

[66] K. Witheephanich, L. Orihuela, R. A. Garcia, and J. M. Escano. Min-max model predictive control with robust zonotope-based observer. In *Proc. of the UKACC 11th IEEE International Conference on Control*, page 1–6, 2016.

[67] G. Zheng, D. Efimov, and W. Perruquetti. Design of interval observer for a class of uncertain unobservable nonlinear systems. *Automatica*, 63:167–174, 2016.